A first-principles study of the structure and lattice dielectric response of $CaCu_3Ti_4O_{12}$

Lixin He, J. B. Neaton, Morrel H. Cohen, and David Vanderbilt
Department of Physics and Astronomy, Rutgers University,
Piscataway, New Jersey 08855-0849

C. C. Homes
Department of Physics, Brookhaven National Laboratory,
Upton, NY 11973-5000

(January 18, 2002)

Structural and electronic properties of $CaCu_3Ti_4O_{12}$ have been calculated using density-functional theory within the local spin-density approximation. After an analysis of structural stability, zone-center optical phonon frequencies are evaluated using the frozen-phonon method, and mode effective charges are determined from computed Berry-phase polarizations. Excellent agreement between calculated and measured phonon frequencies is obtained; calculated mode effective charges are in poorer agreement with experiment, although they are of the correct order of magnitude; and the lattice contribution to the static dielectric constant is calculated to be ∼40. On the basis of these results, various mechanisms are considered for the enormous dielectric response reported in recent experiments. No direct evidence is found for intrinsic lattice or electronic mechanisms, suggesting that increased attention should be given to extrinsic effects.

PACS: 77.84.-s, 63.20.-e, 71.20.-b, 77.22.-d

I. INTRODUCTION

Recently $CaCu_3Ti_4O_{12}$ (CCTO) was discovered to possess one of the largest static dielectric constants ever measured, reaching nearly $\epsilon_0 \sim 80,000$ for single-crystal samples at room temperature.[1–3] Remarkably, the enormous static susceptibility is almost *constant* over a wide temperature range (∼0-500 K). Moreover, measurements of the dynamic susceptibility[3] show that ϵ falls from its huge static value to a more conventional $\epsilon \sim 100$ with increasing frequency, and that this crossover shows a Debye-like frequency dependence (e.g., $\tau^{-1} \simeq 1$ kHz at 80 K) with a relaxation rate τ^{-1} exhibiting an activated dependence on temperature. However, the physical origins of the enormous ϵ_0 and the related Debye relaxation process remain mysterious.

It is tempting to classify a solid exhibiting such a prodigious dielectric response as a relaxor or a ferroelectric, but mounting empirical evidence tends to exclude CCTO from either category. The low-temperature static dielectric response of perovskite ferroelectrics can surpass 1000,[4] rising rapidly above this value with increasing temperature and peaking near the ferroelectric phase transition temperature. However, this peak in response is generally confined to a limited temperature range around the transition, whereas that seen in CCTO appears quite temperature independent (at fixed low frequency) over a much wider range. Furthermore, high-resolution x-ray and neutron powder diffraction measurements on CCTO reveal a centrosymmetric crystal structure (space group $Im3$) persisting down to 35 K, ruling out a conventional ferroelectric phase transition. The Debye-Waller factors are also found to be normal over a wide temperature range, from 35 K to beyond room temperature,[1] inconsistent with random local polar displacements of the magnitude typical in ferroelectrics or their disordered paraelectric phases. Nanodomains or disorder effects, common to relaxor materials, are notably absent: neither superstructure peaks nor strong diffuse scattering are observed in diffraction experiments. Single-crystal samples were described to be mainly twinned, i.e., containing nanoscale domains[1] differing in the sign of the rotation of the TiO_6 octahedra. The presence of the associated domain boundaries may have important consequences for the dielectric properties, as we shall discuss further below.

The crystal structure of CCTO is body-centered cubic with four $ATiO_3$ perovskite-type formula units per primitive cell (where A is either Ca or Cu). The doubled conventional 40-atom unit cell is shown in Fig. 1. The local moments associated with d holes on the Cu^{2+} cations result in the formation of long-range magnetic order; transport, Raman, and neutron diffraction experiments indicate that CCTO is an *antiferromagnetic insulator* having a Néel temperature T_N of 25 K (and Weiss constant $\theta_w = -34$ K).[1,2,5,6] Thus, the 40-atom simple-cubic cell in Fig. 1 is also the primitive cell of the spin structure. Although the extraordinary dielectric behavior persists far above the temperature scale of the magnetic order, the influence of the strongly-correlated local moments, which will likely remain above T_N, is currently unknown.

The purpose of this study is to examine rigorously the ground-state properties of this material using first-principles calculations in order to identify or exclude possible mechanisms underlying the large dielectric response. Our calculations within the local spin-density approximation can serve as an important first step toward the eventual elucidation of this unusual phenomenon. After briefly discussing the technical aspects of our first-

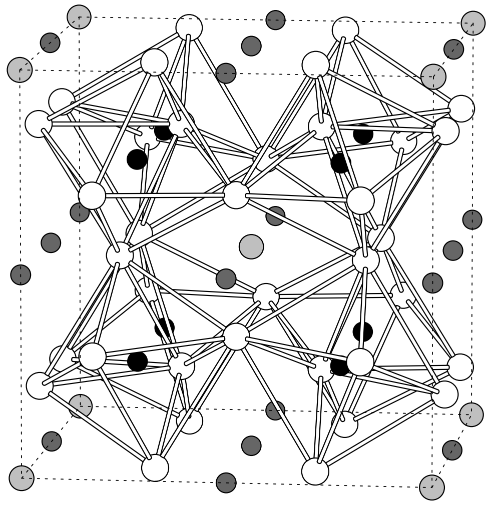

FIG. 1. Structure of $CaCu_3Ti_4O_{12}$ (CCTO), showing tilted oxygen octahedra. White, light, dark, and black atoms are O, Ca, Cu, and Ti respectively. Dashed lines indicate 40-atom primitive cell of antiferromagnetic spin structure.

principles calculations in Sec. II, we provide a detailed analysis of the ground-state structural and electronic properties in Sec. III. In Sec. IV we present the results of frozen-phonon calculations from which we determine the frequencies of the zone-center optical modes. As emphasized below, all modes are found to be stable, consistent with the absence of a structural transition at low temperature. Our calculated frequencies agree well with those measured by Homes *et al.*,[3] although we predict one extra mode apparently absent from their data. The phonon contribution to the static dielectric constant we calculate from first principles does not agree with empirical observation nearly as well as our computed phonon frequencies, but it nonetheless underestimates the measured contribution from the IR-active lattice modes seen in recent experiments ($\sim$80)[3] by a factor less than three. In Sec. V we discuss possible explanations for the observed enormous static dielectric response and associated Debye relaxation behavior, focusing attention on possible extrinsic mechanisms as well as considering intrinsic lattice and electronic mechanisms. We conclude in Sec. VI.

II. METHODOLOGY

To investigate the ground-state structural, electronic, and lattice-dynamical properties of antiferromagnetic CCTO, we employ density functional theory[7] within the local spin-density approximation (LSDA)[8] via the Vienna *ab-initio* Simulations Package (VASP);[9,10] VASP utilizes a plane-wave basis and Vanderbilt ultrasoft pseudopotentials.[11] Our pseudopotentials include nonlinear core corrections[12] and, for Ca and Ti, these potentials treat the highest occupied p shell electrons explicitly as valence; for Cu we also consider electrons in the $3d$ and $4s$ shells self-consistently. A 37 Ry plane-wave cut-off results in convergence of the total energy to 1 meV/ion. The ions are steadily relaxed towards equilibrium until the Hellmann-Feynman forces are less than 10^{-2} eV/Å. When calculating the phonon frequencies, we converge the forces to 10^{-5} eV/Å, resulting in precision of less than 1 cm^{-1}. Brillouin-zone integrations are performed with a Gaussian broadening of 0.1 eV during all relaxations. All calculations are performed with a $2 \times 2 \times 2$ Monkhorst-Pack **k**-point mesh (equivalent to a $4 \times 4 \times 4$ mesh for a single 5-atom perovskite unit cell); doubling the cut-off or the size of the **k**-point mesh does not significantly change the total energy or forces.

TABLE I. Comparison of calculated and measured structural parameters of CCTO. CCTO has space group $Im3$ (point group T_h); the Wyckoff positions are Ca(0, 0, 0), Cu(1/2, 0, 0), Ti(1/4, 1/4, 1/4), O(x, y, 0).

Structural parameter	LSDA	Exp. (35 K)
a (a.u.)	7.290	7.384
x	0.303	0.303
y	0.175	0.179

III. STRUCTURE

The structure of $CaCu_3Ti_4O_{12}$ was first determined from neutron powder-diffraction data over twenty years ago;[13] these results have also been confirmed by more recent neutron-diffraction measurements.[1] The primitive cell is body-centered cubic, with space and point groups $Im3$ and T_h, respectively, and contains 20 atoms; this space group includes inversion symmetry, precluding the possibility of a net spontaneous polarization or ferroelectricity in this structure. Because there are three Cu^{2+} cations in the primitive 20-atom cell, this structure cannot easily accommodate an antiferromagnetic (AFM) spin structure. In fact, neutron diffraction[6] indicates that the AFM state can be described with a doubled 40-atom simple-cubic unit cell as shown in Fig. 1. In this structure, each Cu–Cu nearest-neighbor pair has antiparallel spins. All calculations are performed using this 40-atom cell, although it should be kept in mind that the atomic coordinates and total charge density have the periodicity of the 20-atom bcc cell.

Beginning with the experimental structural parameters, the 40-atom cubic cell is first relaxed for a set of fixed volumes, and the equilibrium lattice constant is then determined by minimizing the total energy as a function of volume. Our calculated lattice constant is $a = 7.290$ Å, less than the value of 7.384 Å measured at 35 K by slightly more than 1%, as is typical in LDA calculations. The internal parameters of the structure are then relaxed at our calculated lattice constant; their values appear in Table I. The stability of the $Im3$ structure is also checked by randomly displacing the ions (lowering the point symmetry from T_h to C_1) and allowing them to relax steadily toward their equilibrium positions. We also randomly displaced the ions *in the same Cartesian direction*, in this case reducing the point symmetry to C_{2v}. Importantly, in both cases the ions returned to their high-symmetry ($Im3$) sites, indicating the absence of unstable (i.e., imaginary-frequency) zone-center optical phonons. (Here we limit ourselves to lattice distortions having the same random displacements in each simple cubic unit cell. Thus both zone-center and (111) zone-boundary instabilities have been investigated for the BCC structure.)

As is evident from Fig. 1, the $Im3$ structure of CCTO can be obtained from an ideal simple-cubic $CaTiO_3$ perovskite by substituting 3/4 of the Ca ions by Cu in a bcc pattern and rotating each TiO_6 octahedron by a fixed angle about one of the four {111} axes. Each Ti ion is then fully coordinated with six equidistant oxygen ions, calculated to be 1.94 Å away. Despite these rotations, the Ca ion continues to possess 12 equidistant oxygen neighbors (calculated distance 2.55 Å) as might be expected for A cations in the ideal perovskite structure. However, the tilted octahedra do result in a radically different local environment for each Cu^{2+} ion: all copper ions are coordinated by a planar arrangement of four nearest-neighbor oxygens (at 1.92 Å) and eight oxygens that are considerably further away. The tilting occurs to relieve tension originating from the relatively small ionic radii of both A-type cations. In this context we note that the ground states of $CaTiO_3$,[14] and to a lesser extent $SrTiO_3$,[15] also exhibit similar octahedral rotations.

IV. ELECTRONIC AND MAGNETIC STRUCTURE

Our calculation of electronic structure, performed on the fully-relaxed geometry, confirms that the ground state is an antiferromagnetic (AFM) insulator (at $T{=}0$) and further illuminates the bonding in CCTO. We find the total charge density to be symmetric, and the spin density to be antisymmetric, under the fractional lattice translation $(a/2, a/2, a/2)$ consistent with the expected AFM state. (Here a is the lattice constant.) We plot the density of single-particle states (DOS) in Fig. 2, calculated within the LSDA for a single spin channel. Both spin channels exhibit identical DOS, as expected for an AFM insulator. The bands in the energy range extending from −7 to 1 eV are mainly O $2p$ and Cu $3d$ in character. The states deeper in these bands, from −7 to−0.5 eV, are found to consist mainly of Cu $3d$ orbitals that hybridize weakly with O $2p$ orbitals that point toward their Ti neighbors. In the range from −0.5 eV to 1 eV we find two narrow bands, each containing just three weakly-dispersive states, composed of strongly σ-antibonding combinations of Cu $3d$ orbitals and O $2p$ orbitals pointing to the Cu from its four near oxygen neighbors (more about this to follow below). The unoccupied conduction-band states above 1 eV in Fig. 2 are primarily Ti $3d$-like, with mainly t_{2g} states making up the bands in the 1-4 eV range and mainly e_g states above 4.5 eV and continuing up to about 7.5 eV.

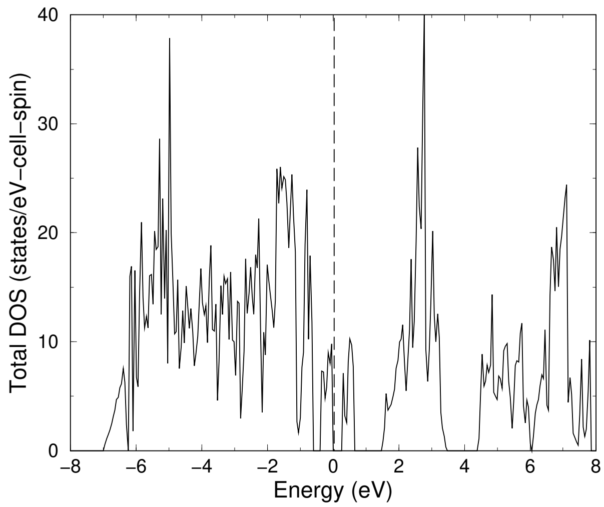

FIG. 2. Density of states (DOS) for CCTO. Spin-up and spin-down DOS are identical, as expected for an antiferromagnet. Vertical dashed line indicates valence-band maximum.

More details are provided in Fig. 3, which affords a magnified view of the total DOS near the fundamental gap and decomposes the DOS into a site-projected partial DOS (PDOS) for the constituent Cu, Ti, and O atoms in the crystal. (The PDOS of Ca is quite small in this energy range.) By symmetry, the total DOS and the Ti PDOS are not spin-polarized, but the spin splitting shows up clearly on Cu and O sites where spin-up and spin-down densities are indicated by solid and dashed curves respectively. Figure 3 clearly illustrates that the fundamental band gap and local magnetic moment arise from the splitting of the six weakly dispersive bands of Cu($3d$)–O($2p$) antibonding orbitals in the −0.5-1 eV energy range.

Further insight about these states can be gained by inspecting Fig. 4, where a contour plot is shown of the spin-up and spin-down charge densities associated with the lower three occupied valence-band states in this group (−0.5-0 eV); a plot for the three unoccupied conduction-band states (0.2-0.7 eV) would look similar but with spins reversed. Figure 4 clearly reveals the Cu($3d$)–O($2p$) σ-antibonding nature of the states, which extend over the central cluster composed of a Cu ion and its four close oxygen neighbors at 1.92 Å (see Sec. III). This cluster evidently forms a strongly spin-polarized unit with a ferromagnetic alignment of the magnetic moments on the Cu and O atoms comprising it, indicating a significant role of the oxygen atoms in the magnetic structure. From the spin densities we estimate the magnetic moment of each CuO_4 complex to be $\sim 0.85\,\mu_B$, where μ_B is the

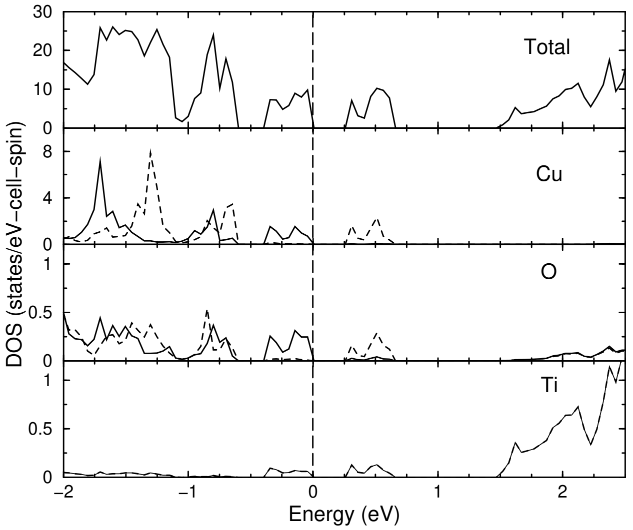

FIG. 3. Total DOS (states/eV-cell-spin) and site-projected partial DOS (PDOS) (states/eV-site-spin) for CCTO. Solid and dashed curves are spin-up and spin-down densities, respectively. Vertical dashed line indicates valence-band maximum. The PDOS is calculated using sphere radii of 0.7 Å, 0.7 Å, and 1.25 Å for Cu, Ti, and O, respectively. The PDOS of Ca, not shown, is very small in this energy range.

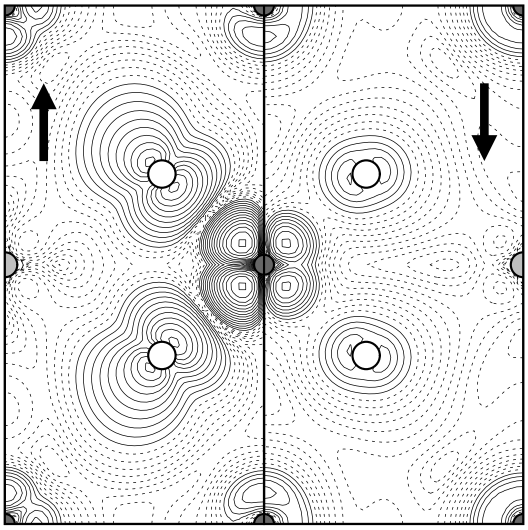

FIG. 4. Spin-up (left panel) and spin-down (right panel) charge densities associated with the three highest occupied valence bands of CCTO plotted with logarithmic contours (five intervals per decade) in the z=0 plane. Each density actually has mirror symmetry across the central dividing line. To facilitate comparison of magnitudes between panels, densities falling below an arbitrary threshold are shown dashed. Atoms are shaded as in Fig. 1.

Bohr magneton; nearly 85% of this moment is derived from electrons in the uppermost three valence bands. A closer examination indicates that each of the four O ions contribute as much as $0.09\,\mu_B$/ion to the total magnetic moment of the CuO_4 unit. The development of such large magnetic moments on oxygen ions has been previously predicted in Li_2CuO_2, a cuprate containing one-dimensional CuO_2 chains.[16] We also note that our calculation compares well with the most recent experimental value of $\sim 0.8\,\mu_B$ extracted from neutron Bragg-peak intensities of CCTO,[6] although less favorably with a previous value of $\sim 0.96\,\mu_B$.[17] Both, however, are significantly larger (by nearly a factor of 2) than moments seen in some undoped cuprates, such as La_2CuO_{4-y},[18] which are notably parent compounds of the doped high-T_c superconductors.

We calculate an indirect band gap of 0.19 eV[19] and a minimum direct gap of 0.27 eV. Our computed gap thus greatly underestimates the experimental optical gap, which must exceed 1.5 eV according to recent data.[20] That the LSDA underestimates the gap dramatically in this case is not particularly surprising; the localized $3d$ orbitals centered on the Cu^{2+} ions will almost certainly result in strong on-site Coulomb interactions, which are not adequately treated at the level of the LSDA. In fact, we expect these interactions to be sufficiently strong that the material is best described as a Mott-Hubbard insulator. In view of this, some additional details of our calculated electronic and magnetic structures should not necessarily be taken at face value. For example, we computed the total energies of the ferromagnetic (FM) and unpolarized paramagnetic (PM) states and found them to be higher than the energy of the AFM ground state by 30 and 60 meV/Cu ion, respectively. Further, both our FM and PM states are *metallic*. Because of the inadequacies of the LSDA, the temptation to use the AFM–FM splitting to estimate the Weiss constant or Néel temperature should be avoided; both would be unphysically large. Moreover, within the conventional picture of a Mott-Hubbard insulator we expect the system to remain insulating, with little change in the optical gap, as the system is switched from an AFM to a FM state, or even as the temperature is raised through the Néel temperature to create a disordered spin state.

Clearly, the LSDA has serious limitations for a system of this kind, and therefore it would be of value to explore the electronic and magnetic structure of this system using more sophisticated many-body tools. One such direction would be along the lines of quasiparticle theory, perhaps using the Bethe-Salpeter extension[21] of the GW theory.[22] An alternative approach could be along the lines of LSDA+U[23] or dynamical mean-field theory (DMFT)[24]. These approaches, which have the capability of taking strong electron-electron interactions into account, would presumably give a more realistic description of the electronic ground state and its excitations in a material such as CCTO.

V. ZONE-CENTER OPTICAL PHONONS

In most insulating perovskites such at $SrTiO_3$ and $CaTiO_3$, the dominant contribution to the static dielectric constant comes from the lattice susceptibility associated with the IR-active phonon modes.[14] Thus, we are strongly motivated to calculate the frequencies and dynamical mode effective charges of these zone-center optical phonon modes, in order to test whether the lattice susceptibility can explain the enormous observed static dielectric constant of CCTO. Moreover, the zone-center optical modes are also of interest in view of some seemingly anomalous behavior observed in the optical IR and Raman spectra as a function of temperature.[2,3] Only ten IR-active modes are observed, despite the fact that the symmetry of the crystal requires eleven distinct IR-active optical phonons. And, perhaps more crucial, the lowest peak, with a frequency of $\sim$122 cm^{-1} at room temperature, shifts to slightly lower frequencies, broadens, and develops a pronounced shoulder as the temperature decreases. Interestingly, the oscillator strength associated with this peak also *increases* by a factor of 3.6, in apparent violation of the f−sum rule. Raman measurements[2] reveal not only three sharp phonon lines, but also some weaker features and a peculiar continuum extending from about 210 to 420 cm^{-1}. It is unclear whether or not these IR and Raman anomalies are connected with the huge static dielectric response, but it is clearly of interest to investigate them as far as possible.

With these motivations in view, we calculate the frequencies of all zone-center optical phonon frequencies in CCTO, and for IR-active modes we also compute the dynamical effective charges needed to evaluate the lattice contribution to the static dielectric constant.

A. Symmetry analysis

Since the Hamiltonian remains invariant under a lattice translation of the 20-atom primitive bcc cell with an accompanying spin reversal, the force constant matrix elements, which are the second derivatives of the total energy with respect to atomic displacements only, are also unchanged. Thus the force-constant matrix has the translational symmetry of the 20-atom cell, and in what follows, we use the symmetry-adapted modes determined from the 20-atom primitive cell (and not the 40-atom conventional cell) in our analysis of zone-center phonons.

To calculate the phonon contribution to the dielectric response, we need only determine frequencies and mode effective charge of the IR-active phonons at the Brillouin-Zone (BZ) center. Altogether there are 60 distinct modes at the Γ point, including the three acoustic (zero-frequency) modes. To minimize the numerical burden, we first decompose these modes into the 6 allowed irreducible representations:

$$\Gamma = 2\mathrm{A}_g \oplus 2\mathrm{E}_g \oplus 4\mathrm{T}_g \oplus 2\mathrm{A}_u \oplus 2\mathrm{E}_u \oplus 12\mathrm{T}_u \qquad (1)$$

Symmetry-adapted modes transforming as each of the irreducible representations given above were constructed using the SMODES symmetry-analysis software package.[25] Among those phonon modes, only the T_u modes are infrared (IR) active; the A_u and E_u are silent, and the remaining modes are Raman active.

B. Zone-center phonon frequencies

For each irreducible representation Γ, we construct an $N_\Gamma \times N_\Gamma$ dynamical matrix from a series of frozen-phonon calculations in which the structure is distorted according to each of the N_Γ symmetry-adapted coordinates consistent with this irreducible representation. For example, for the case of the N_Γ=12 IR-active T_u modes (each of which is three-fold degenerate), we set up a 12×12 dynamical matrix. In all cases, the forces are calculated on the ions in the 40-atom cell and with respect to the correct AFM reference ground state within the LSDA. After calculating the residual Hellmann-Feynman forces F_i^α on ion i and in Cartesian direction α due to displacements u_j^β of ion j in direction β, we displace the ions according to the symmetry coordinate for each mode by 0.1% of lattice constant and recalculate the forces. The force constant matrix

$$\Phi_{ij}^{\alpha\beta} = -\frac{\partial F_i^\alpha}{\partial u_j^\beta} \qquad (2)$$

is then obtained by finite differences by freezing in a small amplitude of each symmetry-adapted distortion pattern that contributes to the modes of a given symmetry and computing the resulting forces that arise. The normal modes $\mathbf{u}_\lambda$ and their frequencies ω_λ are then obtained through solution of the eigenvalue equation

$$\mathbf{\Phi} \cdot \mathbf{u}_\lambda = \omega_\lambda^2 \, \mathbf{M} \cdot \mathbf{u}_\lambda . \qquad (3)$$

Here $M_{ij}^{\alpha\beta} = (m_i/m_0)\,\delta_{ij}\,\delta_{\alpha\beta}$ is the dimensionless diagonal mass matrix, where m_i is the mass of atom i and m_0 is a reference mass chosen here to be 1 amu,[26] and the eigenvectors are normalized according to $\mathbf{u}_\mu \cdot \mathbf{M} \cdot \mathbf{u}_\nu = \delta_{\mu\nu}$.

The results for the IR-active modes are shown in Table II. The overall agreement with experiment[3] is excellent, except for one mode (ω =483 cm^{-1}) apparently missing in the measurement. By symmetry, there should be 11 optical modes (plus 1 acoustic mode) in total, yet only 10 optical modes were observed by experiment. It is possible that the oscillator strength for this mode is immeasurably small; alternatively, its frequency may be so close to that of another mode (ω =507 cm^{-1}) that the pair of modes appears together as a single peak in the optical data. As we show in the next section, however, we compute an appreciable, non-zero oscillator strength for this mode, which is mainly composed of displacements of

TABLE II. Calculated mode frequencies ω_λ, effective charges Z^*_λ, and oscillator strengths $S_\lambda = \Omega_0^2 Z^{*2}_\lambda/\omega_\lambda^2$ of IR-active T_u modes, compared with experimental values extracted from Refs. 3.

ω (cm^{-1})		Z^*_λ		S_λ	
LSDA	Exper.	LSDA	Exper.	LSDA	Exper.
125	122.3	0.51	0.94	4.1	14.3
141	140.8	0.65	1.12	5.4	15.9
160	160.8	0.91	0.84	8.1	6.92
205	198.9	0.55	0.93	1.8	5.25
264	253.9	1.79	1.95	11.5	13.8
314	307.6	0.66	0.52	1.1	0.68
394	382.1	0.36	1.1	0.2	1.96
429	421.0	1.83	1.12	4.6	1.72
483		1.44		2.2	
507	504.2	0.67	0.89	0.4	0.78
563	552.4	0.73	0.88	0.4	0.62

TABLE III. Frequencies (in cm^{-1}) of Raman-active and silent modes of CCTO, with proposed assignments for the three modes observed experimentally in Ref. 2. Irreducible representations are given in parentheses.

	LSDA	Exper.
Raman modes	277 (T_g)	
	292 (E_g)	
	437 (T_g)	
	439 (A_g)	445
	519 (A_g)	513
	552 (T_g)	
	568 (E_g)	577
	739 (T_g)	
Silent modes	123 (E_u)	
	179 (A_u)	
	472 (A_u)	
	490 (E_u)	

Ti and O ions. Furthermore, the sum of the calculated oscillator strengths of the modes at both 483 cm^{-1} and 507 cm^{-1} would greatly exceed that obtained from the observed peak. We return to these inconsistencies below in Sec. VI D.

We also calculate the frequencies of the Raman-active modes and silent modes; the results are listed in Table III. In the case of the Raman modes, we also give proposed assignments of the experimentally observed modes. In the Raman experiment[2] the incident and scattered light were polarized parallel to each other,[27] in which case the symmetry of the Raman tensor requires the intensity of all T_g modes to vanish.[28] The experimental spectrum[2] shows three clear peaks at 445, 513, and 577 cm^{-1}. In addition, there is an anomalous temperature-dependent continuum extending from about 210 to 420 cm^{-1}, on which is superimposed a weak peak at approximately 290 cm^{-1}. Finally, there is also a weak broad peak at approximately 760 cm^{-1}. The three strong peaks are easily assigned as in Table III, and the weak low-frequency peak is almost certainly associated with the E_g mode calculated to lie at 292 cm^{-1}. The feature observed at 760 cm^{-1} could be attributed to the T_g mode computed at 739 cm^{-1} if the assumed polarization alignment was imperfect, allowing some leakage of T_g mode intensity into the spectrum. We cannot directly explain the continuum observed in the 210-420 cm^{-1} range, but note that it could result from a two-phonon Raman process, possibly involving pairs of IR-active modes. Overall, we find excellent agreement between theory and experiment for the frequencies of Raman-active modes.

To summarize, we have computed the frequency of all zone-center modes of CCTO and confirmed that all are stable ($\omega^2 > 0$), consistent with experiments and with our structural relaxation. In particular, our computed ground state is confirmed to be locally stable against all possible ferroelectric lattice distortions.

To test whether the $Im3$ structure is truly a global or only a local minimum, we also calculated the forces and frequencies along the direction defined by some phonon modes at different displacement amplitudes, including the lowest frequency IR phonon. It is found that these phonons remain harmonic for amplitudes up to 4% of the lattice constant. We also examined the possibility of coupling between the low-frequency 122 cm^{-1} mode ($\mathbf{u}_{\rm IR}$) and the Raman modes $\mathbf{u}_{\rm Raman}$ (ω =277cm^{-1} and 292 cm^{-1}), which have frequencies roughly twice that of the lowest-frequency IR mode, to see if multi-phonon processes (i.e., anharmonicity) could explain the anomalies present in the Raman spectrum and optical response measurements. For each of the two lowest-frequency Raman modes, we calculate the total energy versus displacement along two separate directions defined by both $\mathbf{u}_{\rm IR} + \mathbf{u}_{\rm Raman}$ and $\mathbf{u}_{\rm IR} - \mathbf{u}_{\rm Raman}$ combinations of these two modes. Our calculations along these four directions (two associated with each Raman mode) indicate that the total energy is quite quadratic for a wide range of amplitudes (up to 4 % of the lattice constant), indicating that the coupling is too weak among these modes to explain the magnitude of the observed anomalies. Our calculations do not, however, absolutely rule out the possibility of significant coupling between more general combinations of phonons. A more complete stability analysis would require the calculation of the full phonon spectrum; we leave this formidable task for a future investigation.

C. Effective charges and lattice dielectric response

We now turn our attention to a calculation of the lattice contribution to the static dielectric constant, in order to test whether the predicted response is of the correct order of magnitude to explain the enormous observed susceptibility. For this purpose, and also motivated to understand better the observed anomalous temperature dependence of the oscillator strength of the $122\,\mathrm{cm}^{-1}$ mode (see Sec. VI B), we calculate the effective charges of the IR-active modes and their contribution to the dielectric constant. The dielectric function in the frequency range near the lattice vibrations can be written as a sum

$$\epsilon(\omega) = \epsilon_\infty + \epsilon_{\mathrm{ph}}(\omega) \tag{4}$$

of electronic and lattice contributions. In most insulating cubic perovskite oxides (e.g., ferroelectrics and related materials) one has $\epsilon_\infty \sim 5$ and ϵ_0=$\epsilon(0)$ $\sim$20-100, so that the lattice contribution is expected to dominate. It can be written

$$\epsilon_{\mathrm{ph}}(\omega) = {\Omega_0}^2 \sum_\lambda \frac{Z_\lambda^{*\,2}}{{\omega_\lambda}^2 - \omega^2} \; , \tag{5}$$

where ω_λ and Z^*_λ are respectively the mode frequencies and mode dynamical charges, and ${\Omega_0}^2 = 4\pi e^2/m_0 V$ is a characteristic frequency having the interpretation of a plasma frequency of a gas of objects of mass m_0=1 amu,[26] charge e, and density V^{-1} (V is the 20-atom primitive cell volume). Here, we have used the cubic symmetry of CCTO to restrict the sum over λ to just one member of each of the 11 three-fold degenerate sets of IR-active T_u modes, namely the one polarized along z, and the mode dynamical charge is then expressed in terms of atomic dynamical effective charges $Z^*_{i\alpha\beta}$ as

$$Z^*_\lambda = \sum_{i\alpha} Z^*_{i\alpha z}\, u^\alpha_{\lambda i} \; . \tag{6}$$

In practice we compute the mode dynamical charge by finite differences as $Z^*_\lambda = V\Delta P_z/u_0$, where $\Delta P_z = P_z(\mathbf{u}_{\mathrm{eq}} + u_0\,\mathbf{u}_\lambda) - P_z(\mathbf{u}_{\mathrm{eq}})$ and u_0 is a small frozen-ion amplitude of the normal mode $\mathbf{u}_\lambda$ added to the equilibrium position of each ion. ΔP has both ionic and electronic contributions. The ionic contribution is obtained by summing the product of the displacement of each ion with the nominal charge of its rigid core; the electronic contribution is computed from first principles using the Berry-phase theory of polarization.[29] More specifically, the electronic part of the polarization is determined to within a constant (an integer multiple of the polarization "quantum" $e\mathbf{R}/V$, where $\mathbf{R}$ is a lattice vector) by evaluating the phase of the product of overlaps between cell-periodic Bloch functions at successive $\mathbf{k}$-points along a densely-sampled string of points in $\mathbf{k}$-space. This string is chosen so it is parallel to the direction of the desired polarization. For each calculation we use one symmetrized string consisting of 4 $\mathbf{k}$-points (corresponding to 8 $\mathbf{k}$-points/string in a 5-atom perovskite cell). Increasing the number of $\mathbf{k}$-points along the string from 4 to 8 changes the effective charges by less than 1%. The electronic contribution to the polarization is calculated separately for each spin channel; the total polarization is then the sum of the two spin contributions with the ionic contribution.

The calculated mode effective charges are listed in Table II, where they are compared to values obtained from the optical conductivity measurement of Homes *et al.*[3] Surprisingly, though the agreement is excellent between our calculated *frequencies* and those measured at room temperature, the theoretical values of the *mode effective charges* are in poorer agreement with the measured oscillator strengths. That the experimental values refer to room temperature and the computations to 0 K may account for some of the discrepancies, although the large increase measured in the oscillator strength of the lowest-frequency mode at low temperature would compare even less favorably with our calculations. In this context, we note that the measured oscillator strengths are strongly temperature-dependent, while the mode frequencies are only weakly so, suggesting a strong temperature-dependence of the mode effective charges. Because the mode effective charges are essentially electronic quantities, these observations could possibly suggest that the electronic structure of this compound is unusual in some way, and perhaps that this peculiarity is related to the enormous dielectric response. These issues will be discussed further in the next section.

Having these mode effective charges, we estimate the lattice contribution to the static ($\omega \to 0$) dielectric constant $\epsilon_{\mathrm{ph}}(0) = \Omega_0^2 \sum_\lambda Z_\lambda^{*2}/\omega_\lambda^2 = \sum_\lambda S_\lambda$. Using the eigenmodes and their effective charges in Table II, we obtain $\epsilon_{\mathrm{ph}}$$\sim$40 (at zero temperature). Assuming a typical $\epsilon_\infty$$\sim$5-10, we expect $\epsilon_0$$\sim$45-50, to be compared with a sub-IR-frequency dielectric constant of $\sim$70 at room temperature and $\sim$120 at 10 K. Thus despite some detailed disagreement between the experiment and theory for the mode effective charges, the total contribution of these modes to the dielectric constant is of roughly the right order of magnitude in this frequency range.

VI. DISCUSSION AND COMPARISON WITH EXPERIMENT

Although we obtain satisfactory agreement with experiment for computed structural, electronic, magnetic, and lattice-dynamical properties, our calculations *do not* suggest any obvious explanation for either the low-frequency Debye relaxation or its associated enormous static dielectric response. In addition, the observed anomalies associated with the temperature-dependence of the IR and Raman phonons also remain unexplained. The strong T-dependence of the oscillator strength of the lowest-frequency IR-active mode is especially strange. In this section we consider various possible explanations for these distinctive features of CCTO and suggest further experiments that might shed new light on these puzzling phenomena.

A. Possible origins of the large dielectric response and low-frequency Debye relaxation

We consider two classes of possible explanations for the dielectric response and its frequency dependence, one primarily *intrinsic* and one primarily *extrinsic*. By intrinsic, we mean the response that would be measured in a perfectly stoichiometric, defect-free, single-domain crystal of CCTO. Extrinsic effects, on the other hand, would be those associated with defects or other crystal imperfections.

1. Intrinsic mechanisms

We first consider the possibility that the origin of the dielectric response is actually intrinsic, in which case the fact that our calculations do not reproduce the observed behavior could be ascribed to some approximation or restriction of our calculation (e.g., the local spin-density approximation or the fact that we work at zero temperature).

One class of intrinsic origins for the anomolous response would be related to a lattice instability resulting in ferroelectric or relaxor-like behavior. The anomalies recently observed in both the IR and Raman spectra indeed raise the possibility of a close connection between the lattice modes and the enormous dielectric response. Yet, in view of existing experimental evidence and the results of our calculations discussed above, any such connection between the large dielectric response and lattice dynamics cannot be described by simple ferroelectricity. Additionally, there are several specific objections to a relaxor picture, even from a purely experimental point of view. First, relaxors are typically solid solutions (e.g., PMN = $Pb(Mg_{1/3}Nb_{2/3})O_3$) in which the random identity of atoms on one of the sublattices provides an obvious source for disorder. In CCTO the Ca/Cu sublattice is well ordered, and hence there is no obvious source for relaxor-like disorder. Second, it is very hard to reconcile a picture of this kind with the diffraction experiments, all of which fail to observe any of the broadening, superstructure, reduced Bragg intensities, or diffuse background that should be associated with such structural disorder. Third, either the domains are small enough to fluctuate freely in orientation, or they are large enough so that reorientation of their polarization can occur only by domain-wall motion. In the former case, a temperature independent dielectric constant is unlikely. In the latter case, the magnitude of the dielectric constant should be comparable only to that observed in other ferroelectrics containing domains, unless the local polarization is unusually large or the domain-wall mobility monumentally facile.

Moreover, a relaxor picture is difficult to reconcile with our theoretical calculations, since it requires the structure to be unstable to some kind of local polar lattice distortion, and we do not observe such instabilities in our calculations. Of course, one could argue that one of the IR modes really is soft ($\omega^2 < 0$) even though the LSDA calculation indicates otherwise ($\omega^2 > 0$). However, our computed phonon frequencies for the undistorted $Im3$ structure are in excellent agreement with the experimentally observed ones.

Another possible intrinsic origin of the observed dielectric response could be a novel, highly-correlated electronic ground state. Given that CCTO is an antiferromagnetic Mott insulator with an electronic structure containing relatively localized d states as well as dispersive s and p bands, one possibility would be that its anomalous dielectric response could be explained by the formation of *electronic ferroelectricity* (EFE).[30–32] As it is unlikely that the LSDA calculations would correctly describe such a state, our prediction of a conventional antiferromagnetic ground state should not be taken as definitive evidence against this scenario. Nonetheless it can be shown based on symmetry considerations that a *purely* electronic ferroelectric state *is not possible.* In an EFE state, quantities such as the electronic charge density and one-particle density matrix would break the T_h point-group symmetry (and in particular, inversion symmetry). Since the IR-active optical phonons would necessarily couple to such a symmetry breaking, we expect these modes to develop nonzero static mode amplitudes in the EFE state, a result that would be evident in the diffraction or optical spectra (unless the coupling is unusally small).

Several more specific objections to other possible electronic origins can also be raised. First, an electronic instability is most likely in a system with a small gap. However, the experiments suggest that the optical gap in CCTO exceeds 1.5 eV, as would be consistent with the picture of a conventional Mott insulator. It is hard to understand how excitons or other low-frequency excitations could condense in a system with such a robust gap. Second, regarding our theoretical calculations, it is difficult to reconcile our reproduction of the observed phonon frequencies with the inability of the LSDA to reproduce the qualitative nature of the electronic ground state. Third, the Debye relaxation time τ, which is observed to be activated with an attempt frequency in the MHz to GHz range, appears to be too slow to attribute to an electronic mechanism.

2. Extrinsic mechanisms

In view of the experimental and theoretical difficulties with an intrinsic explanation, we observe that many puzzling aspects of the behavior of CCTO become easier to understand if one assumes that the large observed static dielectric response arises from extrinsic mechanisms, such as point, line, or planar defects, or more generally, with sample microstructure, morphology, or boundary layers.

In this case, the intrinsic static dielectric susceptibility would actually be on the order of ~70–120, as is typical for conventional dielectrics in the same structural class.[1] The large response would then be consistent with our theoretical calculations, and with most of the experimental observations (x-ray and neutron diffraction, IR and Raman phonon spectra, etc.) that would effectively observe only the conventional dielectric material. In this scenario, the observed anomalies in the IR and Raman spectra and the huge Debye dielectric response would be completely unrelated phenomena.

Since the dielectric response seems to be too large to be explained by point (or line) defects alone, boundary or interface effects would be needed. There are two obvious candidates for such internal interfaces even in "single-crystal" samples: antiphase boundaries separating regions in which the identity of the Ca sublattice is shifted by a primitive-cubic lattice vector, and twin boundaries separating domains in which the sense of rotation of the oxygen octahedra reverses. Diffraction data[2] does not rule out the occurrence of either kind of domain wall.

If such domain boundaries exist, they could possibly give rise to a large dielectric response as follows. Suppose that, away from such boundaries, CCTO actually has a weak bulk conductivity $\sigma_{\rm b}$ resulting from point defects of some kind. Moreover, assume that the conductance of the sample as a whole is eliminated by the presence of insulating antiphase or twin boundaries that divide the sample into non-percolating, conducting domains. A static dielectric constant on the order of $\epsilon_{\rm ins}/f$ would then be expected, where $\epsilon_{\rm ins}$ is the dielectric constant of the insulating interlayer phase and f is its volume fraction. Assuming $\epsilon_{\rm ins} \sim 10^2$ and $f \sim 10^{-3}$, an overall static dielectric constant of 10^5 is quite plausible. Moreover, the observed *temperature-independence* of this macroscopic response is easily explained as long as $\epsilon_{\rm ins}$ and f do not vary significantly with temperature (in particular, a strongly temperature-dependent $\sigma_{\rm b}$ is allowed). Such a model predicts a Debye relaxation behavior, with a relaxation time τ scaling as $\sigma_{\rm b}^{-1}$, and the observed activated behavior of τ^{-1} is then naturally ascribed to an activated behavior of the intradomain conductivity $\sigma_{\rm b}$.[33] The observed activation energy of 54 meV could be consistent with a variety of mechanisms for such an activated conductivity. For example, one could assume electronic conductivity associated with gap states arising from stoichiometric variations or dopant impurities, or even ionic conductivity associated with mobility of charged defects. This model, which is essentially an elaboration of a suggestion made by Subramanian *et al.* in a "Note added in proof" in their Ref. 1, is worked out in further detail elsewhere[33] for various morphologies of the blocking boundaries, including the possibility that the blocking occurs at the contacts instead of at internal boundaries.

Perhaps the trickiest aspect of such models is that they require the insulating blocking layers to be so uniform and robust that they completely prevent conductivity of the sample as a whole, despite their small volume fraction. One would then expect that small variations in sample preparation procedures might generate samples having enough "holes" in the blocking layers that a measurable conductivity could be observed. In fact, there are hints of such behavior in the experimental work.[27] Further, if the enormous dielectric constant of CCTO does in fact originate from the suggested extrinsic mechanism, the width of the blocking layers, and thence the size of the dielectric response, might be controllable. Accordingly, it would be interesting to explore the internal morphology of single-crystal CCTO samples, both theoretically[33] and experimentally. In this context, we also note that recent studies have uncovered two other new materials, Ca-doped $KTa_{1-x}Nb_xO_3$ (KTN:Ca)[34] and La-doped $PbTiO_3$ (PLT-A)[35], which also exhibit Debye-like relaxation. However, in KTN:Ca this relaxation occurs at temperatures *above* the ferroelectric transition; in PLT-A it occurs at temperatures *below* the ferroelectric transition; and in CCTO it evidently appears in the *absence* of a ferroelectric transition. This would further indicate that the relaxation process is not necessarily related to ferroelectric or relaxor-like behavior at all.

3. Suggestions for experimental tests

Several types of experiments might be useful in testing whether any of the mechanisms proposed above are at work in CCTO. First, it would be interesting to test whether, when looking at sample-dependent variations, one observes any correlation between the behavior of the huge dielectric relaxation (e.g., ϵ_0 values) and properties that are clearly intrinsic (e.g., the oscillator strength of the lowest-frequency IR mode). Such a correlation would tend to rule out an extrinsic mechanism and establish a connection between the phonon anomalies and the huge dielectric response. Second, for samples prepared in such a way as to have a measurable DC conductivity, it would be very interesting to test whether their conductivity is activated in the same way as required to explain the Debye behavior in the macroscopically nonconducting samples. Third, C–V measurements might give strong indications about which type of model is correct. Models based on lattice or electronic ferroelectricity would tend to predict a saturation of the polarization at a characteristic bulk "spontaneous polarization," while the extrinsic models predict a more-or-less linear behavior up to some kind of breakdown voltage. Nonlinearities would reveal the importance of anharmonic effects.

Some other possible avenues of future experimental investigation would be to use electronic probes such as angle-resolved photoemission and inverse photoemission to study the nature of the valence and conduction band edges and to look for unusual quasipartical behavior, or to use optical measurements to characterize the dielectric response in the vicinity of the optical edge. Experiments that could be sensitive to local structural distortions (e.g., EXAFS, nuclear electric quadrupole, etc.) or to glassy dynamics (NMR, spin echo) would also be worth pursuing. An isotope experiment may provide essential evidence for or against a lattice mechanism. Experiments designed to image the assumed domain-boundary blocking layers (e.g., TEM), and to determine their chemical and physical properties, would obviously be of interest.

B. Experimental IR anomalies

We return here to a discussion of the anomalous behavior of the low-frequency peak in the IR response observed by Homes et al.[3] This mode, which appears at $122\,\mathrm{cm}^{-1}$ at room temperature, is observed to broaden and shift to lower frequency ($\sim 115\,\mathrm{cm}^{-1}$ at 10 K) as the temperature is reduced, where it appears to develop a high-frequency shoulder. Most surprisingly, however, its oscillator strength is found to increase by almost a factor of four as the temperature drops from 300 K to 10 K. Moreover, this increase does not seem to be offset by a decrease of oscillator strength of other modes; in fact, the total oscillator strength summed over all IR modes is also observed to rise, growing by $\sim 10\%$ from 300 K to 10 K. This seems especially puzzling since it appears to result in a violation of an oscillator-strength f-sum rule.

To be precise, it is possible to show that, provided there is a good adiabatic separation between the frequency scales of lattice and electronic responses, one expects a sum rule of the form

$$\frac{2}{\pi}\int \mathrm{Im}\,\epsilon(\omega)\,\omega\,d\omega = \Omega_{\mathrm{p}}^2 \tag{7}$$

to hold, where the integral runs over the frequency domain of the lattice modes and

$$\Omega_{\mathrm{p}}^2 = \sum_i \frac{4\pi e^2}{V}\,\frac{\langle Z_i^{*2}\rangle}{M_i} \tag{8}$$

has the interpretation of a "plasma frequency" associated with the ionic charges and masses. Here i runs over atoms in the unit cell of volume V, Z_i^* is the Born effective charge (isotropically averaged[36]) of atom i, and the angle brackets indicate a thermal ensemble average. This result follows directly from the Kramers-Kronig relations and the high-frequency lattice dielectric response $\mathrm{Re}\,\epsilon(\omega) \simeq \epsilon_\infty - \Omega_{\mathrm{p}}^2/\omega^2$ expected in the frequency region above the lattice modes, where the equations of motion are dominated by electric forces and inertia.

The observed strong temperature-dependence of the left-hand side of Eq. (7) need not violate any physical law. Rather, it suggests one of two things. First, it may simply be that the atomic Z^* values are strongly dependent on the local displacements of the atoms, in such a way that the thermal expectation value on the right side of Eq. (7) acquires a strong temperature-dependence. Second, if some kind of continuum of low-frequency electronic excitations extends down to the frequency range of the lattice modes, then the assumptions underlying the derivation of Eq. (7) are not valid. In this case, the electronic structure (at fixed ionic coordinates) might be strongly temperature-dependent in the temperature range of the anomaly.

Our theoretical calculations do not provide any guidance in distinguishing between these possibilities. The second possibility could be suggestive of some kind of electronic mechanism for the enormous dielectric response. However, we note that the temperature and frequency ranges of the IR anomalies are rather different from those of the Debye relaxation, so that such a connection is not necessarily expected. Perhaps careful and precise measurements of $\epsilon(\omega)$ in the frequency range above all phonon modes (i.e., above $750\,\mathrm{cm}^{-1}$) would be the best way of testing whether or not the assumed adiabatic separation between lattice and electronic degrees of freedom really does occur. Additionally, measuring the oscillator strengths as a function of *pressure* may aid in uncovering the nature of the missing mode, as well as providing further information about the anomalous temperature-dependence of the oscillator strengths of the other modes.

VII. CONCLUSIONS

We have performed first-principles calculations within the local-density approximation on $CaCu_3Ti_4O_{12}$ in order to gain insight into the enormous dielectric response reported in recent experiments. Our calculated ground-state structural properties and phonon frequencies agree quite well with preexisting measurements. The electronic structure we calculate appears to underestimate the empirical optical gap in a manner consistent with previous calculations within the LSDA. Our computed effective charges are of the correct order of magnitude or better and result in a lattice contribution to the dielectric constant that is roughly consistent with that observed in the IR range.

While this work does not provide a theoretical explanation for either the Debye relaxation or the unusually large and temperature-independent dielectric response that is observed, our calculations do appear to limit certain intrinsic mechanisms and point toward an extrinsic cause. We find CCTO to be stable in a centrosymmetric crystal structure with space group $Im3$, arguing against the possibility that CCTO is a conventional ferroelectric or relaxor. Our use of the local-density approximation constrains our ability to rule out more unconventional, purely electronic mechanisms, though we note that there is currently no evidence of electronic excitations in the optical spectrum. We also add that there is no experimental support from existing structural or electrical measurements for the large dipole moment, whether electronic or displacive in origin, required in each unit cell to produce the anomalous response. We are unable to provide a quantitative explanation for the changes in oscillator strength of the low-frequency IR-active mode observed in experiment as a function of temperature, although, on the basis of existing measurements, we speculate that it may be uncorrelated with the large dielectric response.

An extrinsic mechanism for the static dielectric response and Debye relaxation has many attractive features. In one version of such a mechanism, a weak conductivity in the interior of domains is barely prevented from leading to a macroscopic bulk conductivity by the presence of then interface blocking layers.[33] In such a scenario, the dielectric susceptibility at and below the Debye response frequency is controlled by this internal conductivity, and is unrelated to lattice distortions, structural phase transitions, or novel electronic states of the crystal. Such a mechanism is then consistent with the absence of diffraction evidence for the kinds of symmetry-lowering distortions expected if a lattice mechanism were at work. It is also consistent with the observation that our computed zone-center phonon frequencies are in excellent agreement with experiment. By the same token, however, such a mechanism cannot explain the observed phonon anomalies, which would have to be attributed to an unrelated cause.

In any case, it is of the utmost importance to clarify which type of mechanism really is responsible for the huge dielectric response and the Debye relaxation behavior in CCTO. For this purpose, the ultimate test must be experimental. We have suggested numerous future avenues of experimental as well as theoretical investigations that could help settle this question. It is our hope that the work described here can serve as a firm theoretical foundation for future investigations of this intriguing material.

ACKNOWLEDGMENTS

This work supported by NSF Grant DMR-9981193. We would like to thank K. M. Rabe for valuable discussions, and also A. P. Ramirez, and S. M. Shapiro for communicating results prior to publication and for useful discussions. We acknowledge M. Marsman for his implementation of the Berry phase technique within VASP. This work is supported, in part, by the U.S. Department of Energy, Division of Materials Science, under Contract No. DE-AC02-98CH10886.

---

[1] M. A. Subramanian, D. Li, N. Duan, B. A. Reisner, and A. W. Sleight, J. Solid State Chem. **151**, 323 (2000).

[2] A. P. Ramirez, M. A. Subramanian, M. Gardel, G. Blumberg, D. Li, T. Vogt, and S. M. Shapiro, Solid State Commun. **115**, 217 (2000).

[3] C. C. Homes, T. Vogt, S. M. Shapiro, S. Wakimoto, and A. P. Ramirez, Science **293**, 673 (2001).

[4] M. E. Lines and A. M. Glass, *Principles and Applications of Ferroelectrics and Related Materials* (Clarendon Press, Oxford, 1977).

[5] A. Koitzsch, G. Blumberg, A. Gozar, B. Dennis, A. P. Ramirez, S. Trebst, and S. Wakimoto, preprint.

[6] Y. J. Kim, S. Wakimoto, S. M. Shapiro, P. M. Gehring, and A. P. Ramirez, preprint.

[7] P. Hohenberg and W. Kohn, Phys. Rev. **136**, 864B (1964).

[8] W. Kohn and L. J. Sham, Phys. Rev. **140**, 1133A (1965).

[9] G. Kresse and J. Hafner, Phys. Rev. B **47**, R558 (1993).

[10] G. Kresse and J. Furthmüller, Phys. Rev. B **54**, 11169 (1996).

[11] D. Vanderbilt, Phys. Rev. B **41**, 7892 (1990).

[12] S. G. Louie, S. Froyen, and M. L. Cohen, Phys. Rev. B **26**, 1738 (1982).

[13] B. Bochu, M. N. Deschizeaux, and J. C. Joubert, J. Solid State Chem. **29**, 291 (1979).

[14] E. Cockayne and B. P. Burton, Phys. Rev. B **62**, 3735 (2000).

[15] N. Sai and D. Vanderbilt, Phys. Rev. B **62**, 13942 (2000).

[16] R. Weht and W. E. Pickett, Phys. Rev. Lett. **81**, 2502 (1998).

[17] A. Collomb, D. Samaras, B. Bochu, and J. C. Joubert, Phys. Stat. Sol. **41**, 459 (1977).

[18] D. Vaknin, S. K. Sinha, D. E. Moncton, D. C. Johnston, J. M. Newsam, C. R. Safinya, and H. E. King, Jr., Phys. Rev. Lett. **58**, 2802 (1987).

[19] The indirect gap is between the high-symmetry points R (the valence band maximum) and X (the conduction band minimum), using the standard notation of the cubic Brillouin zone. The smallest direct gap is at the X point.

[20] C. C. Homes, unpublished.

[21] M. Rohlfing and S. G. Louie, Phys. Rev. Lett. **80**, 3320 (1998).

[22] L. Hedin, Phys. Rev. **139**, A796 (1965); M. S. Hybertsen and S. G. Louie, Phys. Rev. B **34**, 5390 (1986).

[23] V. I. Anisimov, J. Zaanen, and O. K. Andersen, Phys. Rev. B **44**, 943 (1991); V. I. Anisimov, F. Aryasetiawan, A. I. Lichtenstein, J. Phys.: Condens. Matter **9**, 767 (1997).

[24] A. Georges, G. Kotliar, W. Krauth, and M. J. Rozenberg, Rev. Mod. Phys. **68**, 13 (1996).

[25] SMODES was developed by H. T. Stokes and D. M. Hatch. See http://128.187.18.10/~stokesh/smodes.html.

[26] Alternatively, m_0 can be removed from all formulas, in which case Z^*_λ and Ω_0 acquire units of amu$^{-1/2}$ and amu$^{1/2}$ cm^{-1} respectively.

[27] A. Ramirez, private communication.

[28] R. Loudon, Adv. Phys. **13**, 423 (1964); erratum, ibid. **14**, 621 (1965).

[29] R. D. King-Smith and D. Vanderbilt, Phys. Rev. B. **47**, 1651 (1993).

[30] L. M. Falicov and J. C. Kimball, Phys. Rev. Lett. **22**, 997 (1969).

[31] T. Portengen, Th. Östreich, and L. J. Sham, Phys. Rev. Lett. **76**, 3384 (1996); ibid., Phys. Rev. B **54**, 17452 (1996).

[32] G. Czycholl, Phys. Rev. B **59**, 2642 (1999); P. Farkasovsky, Phys. Rev. B **59**, 9707 (1999).
[33] M. H. Cohen *et al.*, to be published.
[34] G. A. Samara and L. A. Boatner, Phys. Rev. B **61**, 3889 (2000).
[35] B. G. Kim, S. M. Cho, T.-Y. Kim, and H. M. Jang, Phys. Rev. Lett. **86**, 3404 (2001).
[36] More precisely, Z_i^{*2} in Eq. (8) should be interpreted as $\frac{1}{3}\sum_\alpha Z_{i\alpha}^{*2}$, where α runs over Cartesian coordinates, and we have made use of the T_h point-group symmetry which insures that $\epsilon_{\alpha\beta}(\omega) = \delta_{\alpha\beta}\,\epsilon(\omega)$.